Journal of the European Ceramic Society **12** (1993) 441–448

Correlation between Casting Parameters and Mechanical Properties of an Al_2O_3–ZrO_2 Composite

C. Galassi, V. Biasini & S. Guicciardi

National Research Council Research Institute for Ceramics Technology, via Granarolo 64, 48018 Faenza, Italy

(Received 3 March 1993; revised version received 3 June 1993; accepted 15 June 1993)

Abstract

Slip casting parameters and mechanical properties were analysed for several different slip casting compositions of tetragonal zirconia–toughened alumina (Al_2O_3–t-ZrO_2). The slurries were prepared with the same weight ratio of the two solid phases, 70/30 for alumina and zirconia respectively, but with a different solid to liquid ratio and different pH of the suspensions. Distinctive features of the green and sintered bodies were shown to be highly dependent on the rheological characteristics of the slurries. Some effects on the final mechanical properties were also found.

Die Gleitgießparameter und die mechanischen Eigenschaften für einige verschiedene Gleitgießzusammensetzungen von tetragonalem, mit Zirkoniumoxid verstärktem Aluminiumoxid (Al_2O_3–t-ZrO_2) wurden untersucht. Die Herstellung des Schlickers erfolgte bei gleichem Gewichtsverhältnis der beiden festen Phasen, 70/30 für Aluminiumoxid beziehungsweise Zirkoniumoxid, aber bei unterschiedlichem Verhältnis von fest–flüssig und unterschiedlichem pH-Wert der Suspensionen. Es konnte gezeigt werden, daß verschiedene Merkmale der Grünlinge und der gesinterten Formen in hohem Maße vom rheologischen Verhalten des Schlickers abhängen. Ebenso zeigten sich Auswirkungen auf die mechanischen Eigenschaften.

Les paramètres pour le moulage en pâte de l'alumine renforçée par de la zircone tétragonale (Al_2O_3–t-ZrO_2), ainsi que ses propriétés mécaniques, ont été étudiés pour différentes compositions de moulage. Les barbotines comportaient la même proportion d'alumine et de zircone (70/30 respectivement), mais la proportion solide–liquide et le pH des suspensions étaient variables. On montre que les caractéristiques des produits bruts et frittés dépendent étroitement des caractéristiques rhéologiques des barbotines. On a également constaté leur influence sur les propriétés mécaniques des produits obtenus.

1 Introduction

Slip casting is a very simple method for shaping complex ceramic components and is a suitable technique for producing green compacts free of defects if proper control of the dispersion properties is maintained. In this respect, powder dispersion, slurry homogenisation and particle packing seem to represent the most crucial steps to obtain green bodies in which large microstructural inhomogeneities are absent.[1–3] In concentrated slurries, powder dispersion is controlled by particle concentration[4] and interparticle interaction. By slip casting tests, it was shown that the higher the slurry concentration, the higher the green density.[5] At any rate, at very high solid content, the interparticle electrostatic repulsive forces alone are not sufficient to keep the particles apart because, at very low interaction distance, the overlapping of the double surface layers produces flocculation in the deep primary minimum of the DLVO theory.[6] To avoid strong flocculation, that promotes particle agglomeration in the green body, the addition of a polyelectrolyte to the suspension is usually needed in order to enhance steric repulsion at a short distance. Of course, electrostatic repulsion is still effective, as evidenced by the change in the rheological behaviour of a suspension when its pH is changed. In the case of binary particulate systems, the dispersion degree must be even more closely controlled to enhance both the highest particle packing in the green body and the most uniform distribution of one phase into the other. A compromise between good dispersion of

Journal of the European Ceramic Society 0955-2219/93/$6.00

the suspension, producing high particle packing, and strong flocculation, that prevents mass segregation, is therefore always necessary.

Due to the difficulty in measuring particle aggregation directly, the assessment of the status of a dispersion is usually made by indirect means. In this context, rheology is a very useful way to get information on the structure and suitability of a slurry for slip casting applications. In fact, as the particle aggregation determines the rheological behaviour of a suspension, the degree of dispersion and/or aggregation can, in principle, be estimated by measuring the rheological parameters of the suspension itself.

In this study, in order to characterise the slip casting behaviour of a composite Al_2O_3–t-ZrO_2 on plaster moulds, highly concentrated suspensions were employed at different solid to liquid ratios. The suspension stability was achieved through an electrosteric mechanism by the addition of a surface-active polymeric ion, lignosulphonate, whose polar part interacts with the solid surface, while the structure of the polymeric chain promotes steric hindrance at very short distances. Since suspension stability increases when adsorption occurs on particles carrying a charge of the same sign as the surface-active agent, in this case a basic pH was chosen to negatively charge the surface of the oxide particles. The pH of the suspensions was also varied for each composition to study its influence on the rheological behaviour. Although the variation of the pH in the chosen range was reported not to influence significantly the ζ-potential at very low particle concentration, its role is critical at very high powder concentrations, as we have demonstrated in separate tests.

The aim of this work is to find a correlation of the rheological parameters of the slip suspensions with the green body texture, as well as the final microstructure and mechanical properties of an Al_2O_3–t-ZrO_2 composite.

2 Experimental Procedures

Commercial powders, Al_2O_3 Alcoa A16 SG (BET specific surface area 10·2 m^2/g) and ZrO_2 Toyosoda TZ-3Y (3 mol% Y_2O_3, BET specific surface area 18·5 m^2/g), were mixed with a ratio of 70/30 in weight (theoretical density of the mix: 4·45 g/cm^3) with the flo-deflocculation procedure shown in Fig. 1. This mixing method[7–9] was shown to give better results than the mechanical route in promoting ZrO_2 dispersion. The casting slurries were prepared by fast stirring the as-prepared powders in de-ionised water with a Na-lignosulphonate deflocculant (Vanisperse CBF-Borregaard) using Al_2O_3 balls as milling

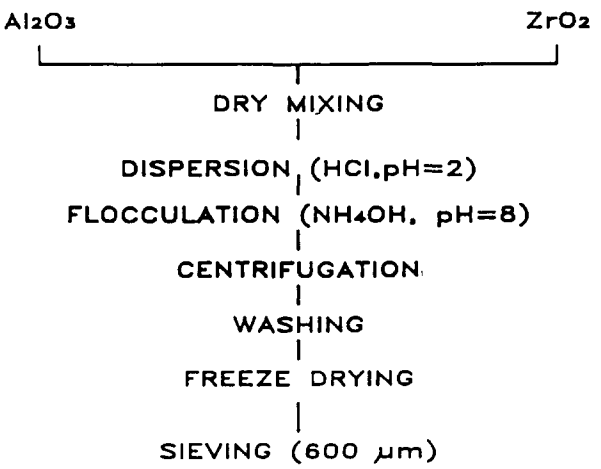

Fig. 1. Flo-deflocculation route for the mixing of the two commercial powders.

media. Three different solid to liquid ratio suspensions were prepared and from each suspension three different slurries were obtained by modification of the pH with ammonia (Table 1). After de-airing, platelet-shaped samples (60 mm × 40 mm × 6 mm) were slip cast in plaster moulds and then sintered in air at 1650°C for 2 h.

The rheological properties (steady-state technique) of the slips were measured with a coaxial cylinder viscometer. Shear stress–shear rate tests were carried out using a Haake RV20 viscometer and the results were analysed using a Bingham model:

$$\tau = \tau_0 + \eta_{pl}\dot{\gamma} \quad (1)$$

where τ is the shear stress (Pa), τ_0 is the extrapolated yield stress at $\dot{\gamma} = 0$ (Pa), η_{pl} is the apparent or plastic viscosity (Pa s) and $\dot{\gamma}$ is the shear rate (s^{-1}). Density and porosity were measured by mercury intrusion (Porosimeter 2000, Carlo Erba). The morphology of the green bodies was evaluated by scanning electron microscopy (SEM) (Cambridge Stereoscan 360). On the sintered samples, the density was measured using the Archimedean principle. SEM and X-ray (Geigerflex, Rigaku) analyses were performed on polished surfaces, fracture surfaces and thermal etched surfaces (1440°C in air for 30 min). The mean grain

Table 1. Composition and pH values of the slurries

System	*Solid phase*		*Deflocculant* (*wt%*)	*pH*
	(*wt%*)	(*vol.%*)		
A1	70	34	0·6	9·3
A2	70	34	0·6	10·0
A3	70	34	0·6	10·6
B1	75	40	0·6	9·3
B2	75	40	0·6	10·0
B3	75	40	0·6	10·6
C1	77	43	0·6	9·3
C2	77	43	0·6	10·0
C3	77	43	0·6	10·6

size was calculated by Hilliard's method.[10] Young's modulus (E), Vickers microhardness (HV), flexural strength (σ) and fracture toughness (K_{Ic}) were measured for most of the systems. Young's modulus was calculated using the resonant frequency method.[11] The microhardness (Zwick 3212) was measured with a load of 4·91 N. The flexural strength (Instron mod. 1195) was measured on a four-point bending fixture with an outer and inner span of 40 and 20 mm, respectively. The bars, 45 mm × 4 mm × 3 mm, were fractured with a crosshead speed of 0·5 mm/min. The tensile faces of the bars were previously machined and then diamond paste polished down to 1 μm. The edges of the tensile face were bevelled. The fracture toughness was measured by the chevron notched bar (CNB) technique[12] on a four-point fixture with an outer and an inner span of 26 and 13 mm, respectively. The samples were fractured with a crosshead speed of 0·05 mm/min.

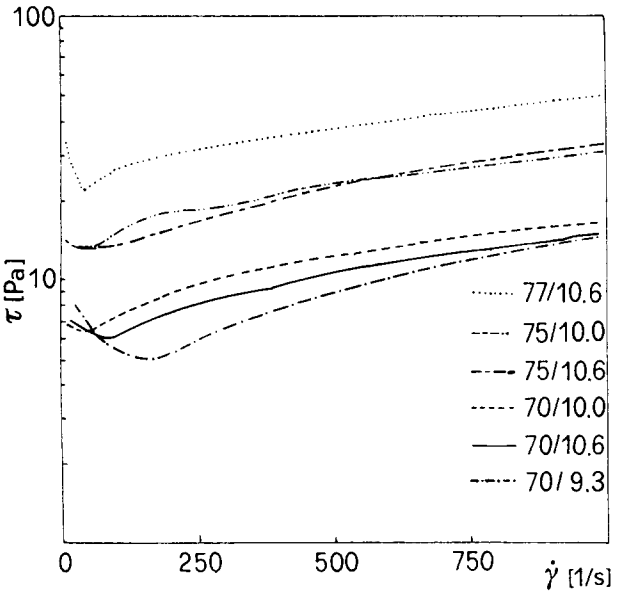

Fig. 2. Flow curve of the suspensions suitable for slip casting tests at an increasing shear rate. Curve labels are solid content (%) and pH, respectively.

3 Results and Discussion

3.1 Rheological behaviour

In this study, the rheological behaviour of the suspensions was evaluated at a constant shear rate of $10\,s^{-1}$, which is reported to be a shear rate that simulates the flow conditions in slip casting tests. The flow curves were also recorded at higher shear rate, increasing the shear rate up to $1000\,s^{-1}$ and then returning to zero, so as to make uneffective the interactions and just observe the flow of the non-interacting primary kinetic units.

In these tests, most of the slurries showed a typical pseudo-plastic flow curve (Fig. 2 and Table 2), with a yield value which was more and more evident as the solid content was increased. Several systems showed a time-dependent behaviour that was more pronounced as the solid content increased. Moreover, on increasing the solid content, the slurry became more fluid with the increase of the pH (Table 2, Fig. 3). At high solid contents and low pH values, some slurries were too thick to be castable (Table 2) like samples B1 and C2, or, as in the case of sample C1, definitely inadequate. Due to their unsuitable slip casting behaviour, these systems were not characterised further. From the values of viscosity at low shear rate, it is possible to see that, with the solid content, the pH also had to be increased to maintain the slurry viscosity in a range useful for slip casting (Table 2). Usually, the optimum value of η is considered to be some 1 Pa s, but the slurry C3 was considered to be still castable.

When considering the rheological behaviour of a suspension, shear thinning and time-dependent effects are normally related to the formation kinetics of particle aggregates, called flocs, floc deformation and floc disaggregation. Of course, the contribution to the rheological behaviour of the suspension from one of these three events will be different depending on the shear rate imposed during the test.[13] At high shear rates, from the linear part of the flow curves (Fig. 2) the plastic velocity, η_{pl}, was calculated for

Table 2. Rheological parameters

System	*Rheological behaviour*[a]	τ_0[b] *(Pa)*	η[c] *(Pa s)*	η_{pl} *(10^{-2} Pa s)*	ϕ_n	ϕ_{eff}	C_{fp}
A1	P	3·1	0·6	1·14	0·34	0·56	1·66
A2	T	6·1	0·3	1·04	0·34	0·55	1·62
A3	T	5·8	0·3	0·92	0·34	0·54	1·58
B1	R	—	4·1	4·4	0·40	—	—
B2	T	14·6	1·3	1·60	0·40	0·60	1·50
B3	P	11·2	1·3	2·20	0·40	0·63	1·57
C1	—	—	—	—	0·43	—	—
C2	R	—	4·4	6·9	0·43	—	—
C3	P	25·1	2·8	2·45	0·43	0·64	1·48

[a] P, Pseudoplastic; T, Tixotropic; R, Rheopectic.
[b] Extrapolated value.
[c] At $\dot{\gamma} = 10\,s^{-1}$.

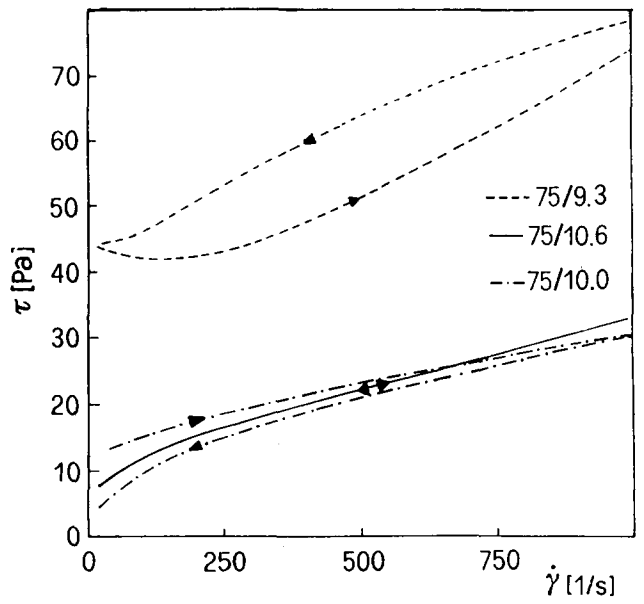

Fig. 3. Up- and down-flow curves for the suspension B at different pH values. Curve labels are solid content (%) and pH, respectively.

each system with eqn (1) (see Table 2). When time-dependent effects were present, η_{pl} was calculated in the linear portion of the curve measured at increasing shear rate. From the η_{pl} values, it is possible to estimate the effective volume fraction, ϕ_{eff}, occupied by the solid phase in the suspension that depends on the interparticle interaction and the structure of the kinetic unit. ϕ_{eff} was calculated according to the Quemada equation:[14]

$$\eta_r = (1 - 1{\cdot}25\phi_{eff})^{-2} \quad (2)$$

where η_r is the relative viscosity, i.e. $\eta_r = \eta_{pl}/\eta_0$ where η_{pl} is the observed viscosity and η_0 is the viscosity of the dispersing medium ($\eta_0 = 1$ m MPa s, in this case as the dispersing medium was water). Dividing ϕ_{eff} by ϕ_n, the nominal volume fraction, the disperse phase volume increment, C_{fp}, also called flock bulkiness, is obtained (Table 2). C_{fp} is an indicator of the status of the particle aggregation: the higher the C_{fp}, the lower the density of the flocks.

From the values of C_{fp}, it is evident that all the systems underwent some degree of flocculation since all their C_{fp} values are >1 that is the expected value when the kinetic units are primary particles. This flocculation was certainly due to the very high concentration of oxide particles with different chemical composition in the slurry. In the investigated pH range, all the oxide particles are negatively charged but for two of them, alumina and yttria, these conditions are quite close to their isoelectric point (IEP), i.e. pH $\cong$ 9·2.[15,16] In this range of pH, in the absence of any deflocculant and in dilute suspensions, the ζ-potential of the three oxide powders does not reach high absolute values (they are all in the range -5 to -30 mV) and this electrostatic similarity could have favoured a non-uniform distribution of these different oxide particles when mixed.[17] A contribution to the flocculation can moreover be ascribed to the presence of yttria in the zirconia powder which promotes similarity of the zirconia to the alumina particles.[18]

As mentioned in the introduction, the density of a slip-cast green body increases with the solid volume fraction in the slurry. As in the present case, for systems A, B and C, the control of the electrostatic repulsive forces alone was known not to be effective in preventing strong flocculation, we tried to avoid this flocculation through the adsorption of the polyelectrolyte on the particle surfaces to promote steric hindrance.[19] Although effective in improving the solid volume fraction in the slurry (see Table 2) the conditions chosen in this study were nevertheless not always suitable to prevent the formation, by heteroflocculation, of some oxide clusters which were found in several green and sintered samples, as we will describe later.

3.2 Green and sintered samples

In Table 3, the green density, the final density and the mean grain size of the matrix are reported for each system.

The low values of green density confirmed the presence of agglomerates due to the heteroflocculation of the slurries which hampered good particle packing. Generally, the green density increased with the solid load of the slurry. A direct relationship of the green density versus the bulkiness of the flock, C_{fp}, was not evident (Fig. 4) even though a clear tendency to decrease the green density with the increase of C_{fp} can be noted.

Modification of pH from 9·3, the value of the as-prepared slurry, to 10·6, with ammonia, was critical for reducing viscosity and, consequently, for improving the solid volume fraction in the slurry, see system C in Table 2. On the other hand, for a given volume fraction (34 vol.%), the increase of the pH to 10·6 was detrimental and produced the worst texture among the green samples, as will be shown later. This could be explained by taking into account the variation of the ratio of the ζ-potential of the two oxides. A pH value of 9·3 is near the IEP of alumina and far

Table 3. Density and matrix grain size of the composites

System	*Density (% theoretical density)*		*Grain size (μm)*
	Green	*Sintered*	
A1	51·6	99·1	0·93
A2	51·1	98·6	0·88
A3	55·9	96·9	0·92
B2	54·3	96·8	1·06
B3	54·0	98·3	0·80
C3	55·0	99·5	0·99

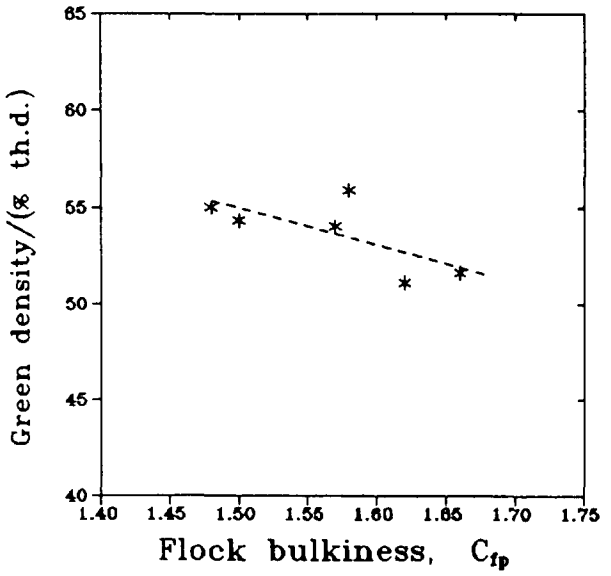

Fig. 4. Green density versus flock bulkiness. The dashed curve is the best fit of the data.

from the IEP of zirconia that is between 6 and 7.[18] As evidenced by Bleier and Westmoreland,[17] the higher the ratio of the ζ-potentials the better the distribution of the secondary phase in the matrix. In our case, the measured values were $\zeta \cong -30\,mV$ for the ZrO_2 TZ-3Y powder and $\zeta \cong -5\,mV$ for the Al_2O_3 Alcoa A16 powder, respectively. In spite of the high value of the ratio of the two ζ-potentials, due to their low absolute values at this value of pH, the green density of sample A1 was rather low owing to the presence of large flocs as evidenced by the largest value of C_{fp} (see Table 2). At the same volume fraction, 34 vol.% the increase in the pH to 10·6 promoted an overall better particle packing (the C_{fp} was smaller and the green density was the highest among the samples produced, see Tables 2 and 3) but larger agglomerates were retained in the body due to the lower ratio of the ζ-potentials. The morphological analysis of the green samples confirmed that in this condition few large agglomerates were effectively present (Figs 5(a)–(c)).

Independently of the starting green density, high values ($\geq 99\%$) of final density were measured only for the samples produced with the pseudoplastic suspensions: A1, B3 and C3.

In all the sintered samples, large areas with a uniform distribution of Al_2O_3 and ZrO_2 grains were present. In these areas (Fig. 6) the sintered bodies showed a microstructure in which ZrO_2 grains fill the interstices between Al_2O_3 grains. It confirms the effectiveness of the flo-deflocculation route shown in Fig. 1 to produce a good dispersion of ZrO_2 particles in the alumina matrix: the powder mix is dried starting from a flocked suspension with a pH in the range between the two IEP when the two oxide powders present a surface charge of opposite sign. The best distribution of the two phases seems to be achieved at the expenses of green density, i.e.

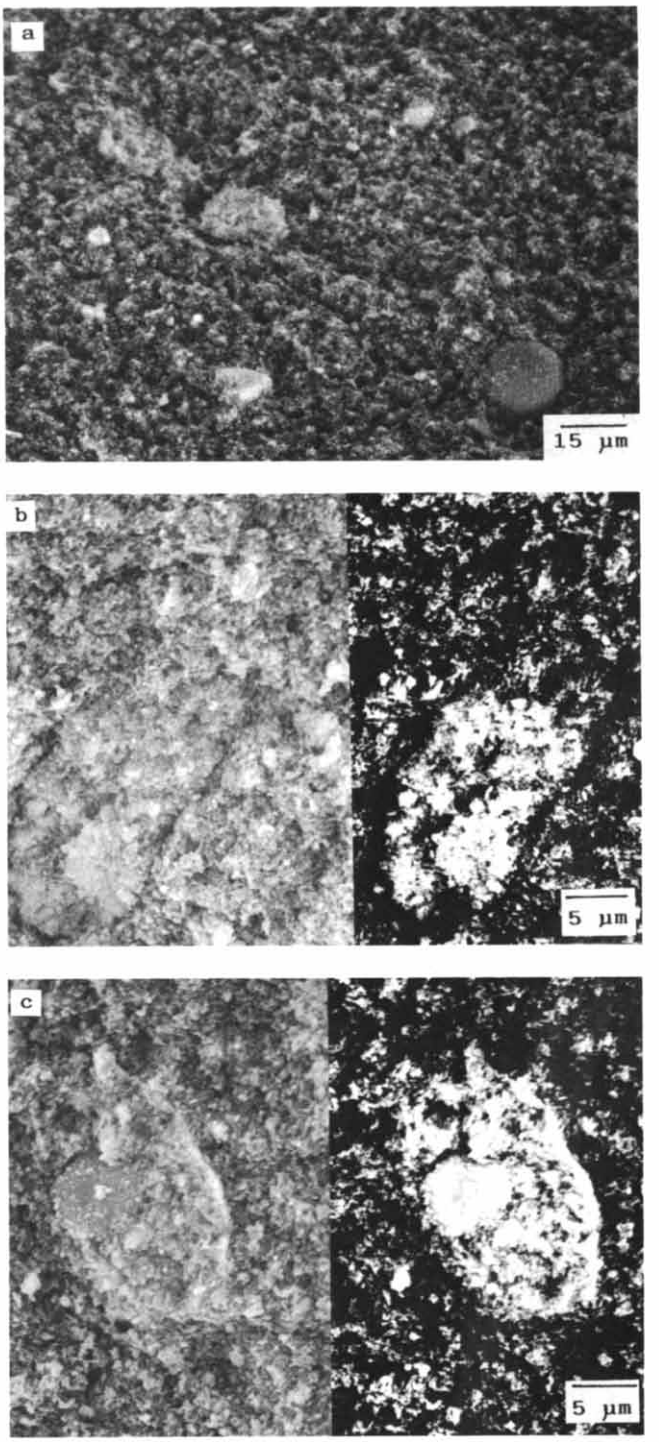

Fig. 5. SEM micrographs showing (a) the presence of agglomerates in the green bodies, (b) and (c) their zirconia-based composition (BSE image).

samples A1 and A2. The best microstructure was found in sample A1 (Fig. 7(a)) with very few clusters and low porosity, while the worst microstructure was shown by sample A3 (Fig. 7(b)) where, besides the clusters, a lot of crack-like voids and some small pores between or inside the ZrO_2 grain clusters were observed. ZrO_2 agglomerates were distributed in the Al_2O_3 matrixes in different amounts and morphology depending on the rheological characteristics of the slurry. In the sintered bodies, the segregation voids between the clusters shown in Fig. 6 remained in

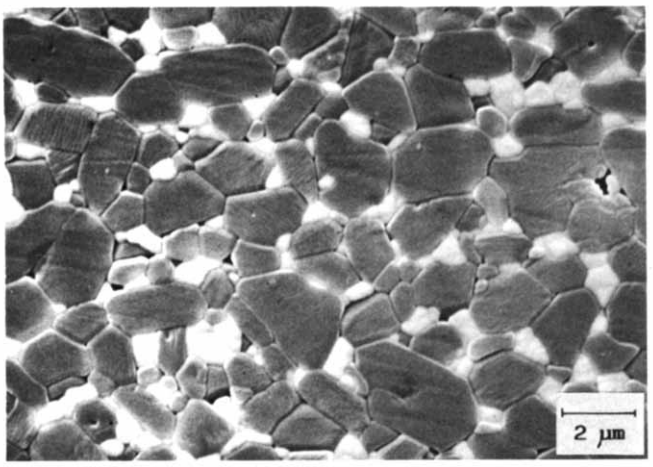

Fig. 6. SEM micrograph showing the good general distribution of zirconia grains in the alumina matrix (sample A2).

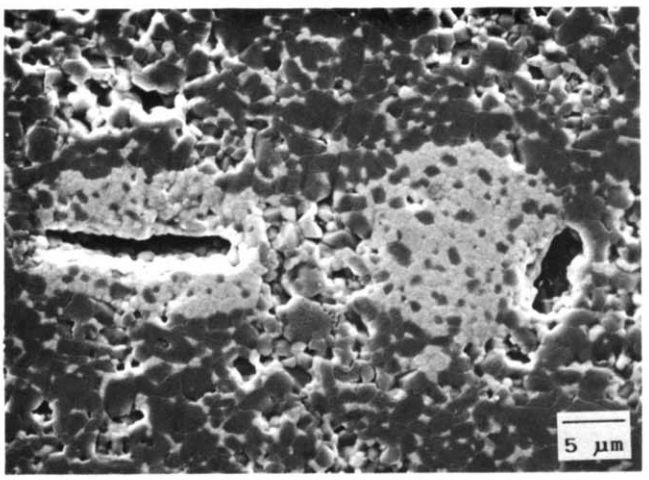

Fig. 8. SEM micrograph showing some kinds of voids that accompany ZrO_2 aggregates after sintering.

the form of elongated or circular fissures (Fig. 8). ZrO_2 agglomerates give rise to first generation pores (within clusters) and second generation pores (between the clusters) mostly in the form of crack-like voids, with dimensions up to 20 μm. It is well known that well distributed zirconia added to alumina acts, during sintering, primarily as the agent hindering the grain growth of the matrix material. In our case, the mean grain size ranged from $\sim$0·8 to $\sim$1·1 μm. In the cases of the best ZrO_2 distribution (samples A1, A2 and B3), i.e. with dominantly singular ZrO_2 particles at the Al_2O_3 triple points, the smallest matrix grain size was measured (in areas not affected by clusters and/or other defects). When ZrO_2 particles were irregularly concentrated in small aggregates through the matrix (sample B2, Fig. 9), some grain growth was observed. Two samples, A3 and B2, evidenced poor microstructural characteristics: a higher number of ZrO_2 clusters with crack-like voids between or inside the clusters and a high amount of smaller porosity.

As evidenced by X-ray analysis, zirconia was retained in the tetragonal form both after sintering and machining followed by polishing.

3.3 Mechanical properties

The values of the mechanical properties are reported, for each system, in Table 4, with mean and standard deviation where appropriate.

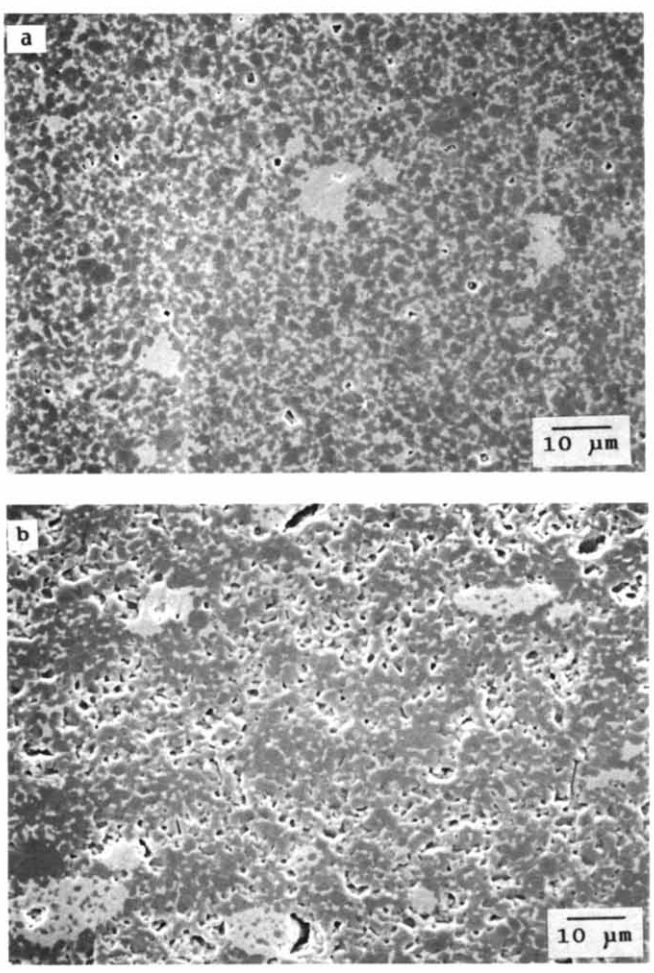

Fig. 7. SEM micrographs of (a) the best microstructure (sample A1), and (b) the worst microstructure (sample A3) after sintering.

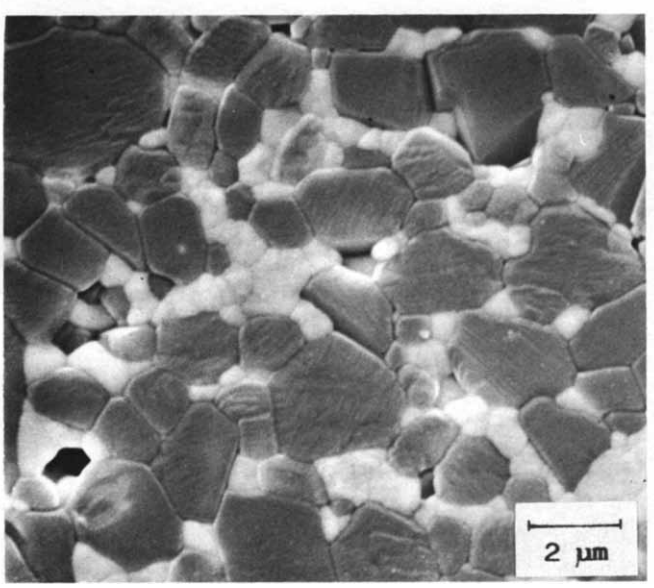

Fig. 9. SEM micrograph showing grain growth of alumina owing to a non-uniform distribution of zirconia phase.

Table 4. Mechanical properties

System	*E* (*GPa*)	*Hv* 0·5 (*GPa*)	σ (*MPa*)	K_{Ic} ($MPa\sqrt{m}$)	c^a (μm)
A1	344 ± 5	17·1 ± 0·4	613 ± 37	4·86 ± 0·38	40
A2	348 ± 5	17·5 ± 0·3	586 ± 42	4·60 ± 0·18	40
A3	347 ± 1	17·4 ± 0·4	483 ± 100	4·57 ± 0·04	58
B2	353 ± 3	16·7 ± 0·3	489 ± 42	4·73 ± 0·12	61
B3	349 ± 5	17·7 ± 1·3	581 ± 133	4·57 ± 0·31	40
C3	350 ± 3	17·7 ± 0·3	507 ± 96	4·62 ± 0·15	54

[a] Critical flaw size.

For the Young's modulus, no particular difference was found among the systems. Our experimental values are in good agreement with those reported by Lange.[20] For a two-phase composite, it is possible to approximately calculate the upper and lower bounds within which the experimental values of E should fall.[21] Taking 396 and 235 as Young's modulus for Al_2O_3 (Ref. 22) and ZrO_2 (Ref. 23), respectively, the upper and lower bounds are 363 and 343 GPa, respectively. As can be seen in Table 4, the experimental values are within the calculated bounds, and, generally, very close to the lower one, as expected in the case of a particulate composite.[21] That the experimental values are inside the calculated bounds indicates that the samples were not affected by a significant presence of porosity or microcracking. In their work, Konsztowicz and Whiteway[24] have reported that in Al_2O_3–ZrO_2 composites prepared by slip casting some microcracks were present due to the different thermal expansion of the ZrO_2 agglomerates with respect to the matrix and that, moreover, some agglomerates were detached from the matrix. The agglomerates behaved, in this way, as large pores. Our experimental results for Young's modulus do not exclude the possibility of such defects; they only indicate that their number was not so large as to be revealed by the Young's modulus measurements that is known to be sensitive to the presence of pores[25] or microcracks.[26]

With respect to microhardness, the systems show some little differences. Taking into account the experimental dispersions, the value of microhardness is almost the same in most cases. For a similar Al_2O_3–ZrO_2 composite, Lange[20] reported hardness values lower than ours, but he used a higher indentation load. The system B2 shows a value that is substantially lower than the others, probably due to its low relative density and larger grain size (Table 3). Sample B3 has a hardness value close to the general mean but it has also the largest standard deviation. It is likely that in this case, few large zirconia-containing areas were tested by the indentor. Since the zirconia phase is softer than the matrix, the resulting microhardness dispersion could have been negatively affected.

The values of K_{Ic} we measured are nearly the same for all the systems and very close to those reported by Becher and Tennery.[27]

Some evident differences emerged regarding the flexural strength among the systems, and are clearly linked to the microstructural characteristics of the composites, which are in turn dependent on the slurry characteristics. In fact, it is well known that during sintering the intergranular pores are easy to rearrange. On the other hand, big intra-cluster pores, inter-clusters fissures and porosity that derive from the inefficient packing of particulate clusters remain after sintering and are deleterious for mechanical properties. In our case, the best flexural strength value was observed for sample A1, containing a low amount of solid phase and with the slurry showing a pseudoplastic behaviour. Relatively good strength values were also measured for sample A2, which has the best distribution of ZrO_2 particles around the Al_2O_3 grains, and for sample B3. On the other hand, a significant decline in strength was observed for samples A3 and B2, which have a high quantity of defects and total porosity. For all the systems, the principal strength-determining factors were the crack-like voids present in the microstructure, mainly for the systems A3, B2 and C3. Using the Griffith formula for the strength of a brittle material:[28]

$$\sigma = Y \frac{K_{Ic}}{\sqrt{\pi c}} \tag{3}$$

where σ is the mean strength (MPa), Y a geometrical factor, K_{Ic} the fracture toughness ($MPa\sqrt{m}$) and c the mean size of the fracture-originating flaw (m), it is possible to calculate the mean size of the defect that induced the failure in our samples. Column 6 of Table 4 reports the critical flaw size calculated in this way taking a value of 1·43 for Y, which corresponds to a penny-shaped surface crack.[29] As can be seen, the mean critical flaw size was much larger than any microstructural feature found in the materials. A possible explanation is that the fracture-initiating defect could have subcritically grown during loading. Such a phenomenon is known to be active in these materials[30] even if the value of n (the stress intensity exponent in the relation $v = AK_I^n$) there

reported is not characteristic of a material very sensitive to fatigue. Another explanation could be that a synergetic mechanism acted when some defects were close to each other as shown in Fig. 8. In particularly low-strength samples, the fracture origins were very large pores ($\approx 100\,\mu m$) which probably remained in the slurry after de-airing.

4 Conclusions

In this study, the relationships between the suspension characteristics and the green and sintered body properties of an Al_2O_3–ZrO_2 composite material produced by slip casting were examined.

The dispersions were produced starting with two commercial powders mixed through a flo-deflocculation route with the addition of a polyelectrolyte. In these dispersions, the pH and the solid volume fraction were varied to assess their influence on the rheological behaviour. Correlations between the floc bulkiness and the green density and texture were evidenced and explained in terms of pH effects on the ζ-potentials. High pH values were shown to allow maximum solid loading. In the sintered bodies, the zirconia distribution was generally found to be uniform through the thickness of the bodies. Anyway, heteroflocculation could not be avoided and some zirconia agglomerates were still present in the sintered bodies in an amount that increased with the gains in the solid volume fraction and the pH. Most of the mechanical properties, i.e. Young's modulus, hardness and fracture toughness, of the sintered bodies were only slightly influenced by the rheological features of the dispersions. Instead, the flexural strength was related to the dispersion properties as the fracture origins were microstructural defects such as zirconia agglomerates and large pores.

References

1. McLean, A. F., Ceramic technology for automotive turbines. *Am. Ceram. Soc. Bull.*, **61** (1982) 861–71.
2. Phelps, G. W., *Slip Casting*. Interceram-Ceramic monographs 1.4.2, Verlag Schmid, Freiburg, Germany, 1982, pp. 1–9.
3. Aksay, I. A., Microstructure control through colloidal consolidation. *Adv. Ceram.*, **9** (1984) 94–104.
4. Ottewill, R. H., *Properties of Concentrated Dispersions in Solid/Liquid Dispersions*, ed. Th. F. Tadros. Academic Press, London, UK, 1987, pp. 183–98.
5. Galassi, C., Roncari, E., Capiani, C. & Piancastelli, A., Slip rheology correlated to green and sintered ZrO_2 properties. In *Proceedings of the 2nd ECERS Conference*, Ausburg, 1991, ed. G. Ziegler and H. Hausner, Deutsche Keramische Gesellschaft, Cologne, Germany (in press).
6. Hiemenz, P. C., *Principles of Colloid and Surface Chemistry* (2nd edn). Marcel Dekker, New York, USA, 1986, pp. 677–731.
7. Bellosi, A., Galassi, C. & Guicciardi, S., Slip casting of Al_2O_3 and Al_2O_3/ZrO_2 composites. *J. Mater. Sci.*, **25** (1990) 4331–40.
8. Aksay, I. A., Lange, F. F. & Davis, B. I., Uniformity of Al_2O_3/ZrO_2 composites by colloidal filtration. *J. Am. Ceram. Soc.*, **66** (1983) C190–C192.
9. Galassi, C., Roncari, E., Capiani, C. & Piancastelli, A., Evaluation of green bodies related to the forming technique. *EURO-CERAMICS vol. 1—Processing of Ceramics*, ed. G. de With, R. A. Terpstra & R. Metselaar. Elsevier Applied Science, London, UK, 1989.
10. Hilliard, J. E., General Electric Research Laboratory Report No. 62-RL-3133M, Schenectady, New York, December 1962. *Metal Prog.*, **85** (1964) 99.
11. Standard method for Young's modulus, shear modulus and Poisson ratio for ceramic whitewares by resonance, ASTM C 848-78 (reapproved 1983). American Society for Testing and Materials, Philadelphia, USA.
12. Munz, D. G., Shannon, J. L. & Bubsey, R. T., Fracture toughness calculation from maximum load in four point bend tests of chevron notch specimens. *Int. J. of Fracture*, **16** (1980) R137–41.
13. Kuno, H. & Senna, M., A practical analysis of pseudoplastic flow suspensions. *J. Colloid. Interface Sci.*, **57** (1976) 248–56.
14. Quemada, D., *Rheol. Acta*, **17** (1978) 632.
15. Deliso, E. M., Srinivasa Rao, A. & Cannon, W. R., Electrokinetic behaviour of Al_2O_3 and ZrO_2 powders in dilute and concentrated aqueous dispersions. *Adv. Ceram.*, **21** (1987) 525–35.
16. Parks, G. A., The isoelectric points of solid oxides, solid hydroxides and aqueous hydroxo complex systems. *Chem. Rev.*, **65** (1965) 177–96.
17. Bleier, A. & Westmorland, C. G., Effects of pH and particle size on the processing of and the development of microstructure in alumina–zirconia composites. *J. Am. Ceram. Soc.*, **74** (1991) 3100–11.
18. Goski, D. T., Kwack, J. C. & Konsztowicz, K. J., The effect of yttria stabiliser on electrokinetic behaviour of ZrO_2–Al_2O_3 colloidal suspensions. *Ceram. Trans.*, **26** (1991) 24.
19. Tadros, Th. F., *Solid–Liquid Dispersions*. Academic Press, London, UK, 1987.
20. Lange, F. F., Transformation toughening: IV, fabrication, fracture toughness and strength of Al_2O_3–ZrO_2 composite. *J. Mater. Sci.*, **17** (1982) 247–54.
21. Ashby, M. F. & Jones, D. R. H., *Engineering Materials*. Pergamon Press, Oxford, UK, 1980.
22. Dörre, E. & Hübner, H., *Alumina*. Springer-Verlag, Berlin, Germany, 1984.
23. Ishitsuka, M., Sato, T., Eudo, T. & Shimada, M., Sintering and mechanical properties of yttria-doped tetragonal ZrO_2 polycrystal/mullite composites. *J. Am. Ceram. Soc.*, **70** (1987) C342–C346.
24. Konsztowicz, K. J. & Witheway, S. G., Processing contribution to microcrack formation in ZTA composites. *Ceram. Engng Proc.*, **11** (1990) 1405–22.
25. Boch, P. & Glandus, J. C., Porosity effects on mechanical properties of ceramics. *Interceram.*, **3** (1983) 33–6.
26. Budiansky, B. & O'Connell, R. J., Elastic moduli of a cracked solid. *Int. J. Solids Struct.*, **12** (1976) 81–97.
27. Becher, P. F. & Tennery, V. J., Fracture toughness of Al_2O_3–ZrO_2 composites. In *Fracture Mechanics of Ceramics* (Vol. 6), ed. R. C. Bradt, A. G. Evans, D. P. H. Hasselmann & F. F. Lange. Plenum, New York, USA, 1983, pp. 383–9.
28. Griffith, A. A., The phenomena of rupture and flow in solids. *Phil. Trans. Royal Soc. London*, **A221** (1920) 163.
29. Atkins, A. G. & Mai, Y.-W., *Elastic and Plastic Fracture*. Ellis Horwood Ltd, Chichester, UK, 1988.
30. Orange, G., Fantozzi, G., Homerin, P., Thevenot, F., Leriche, A. & Cambier, F., Preparation and characterization of a dispersion toughened ceramic for thermomechanical uses (ZTA). Part II: thermomechanical characterization. Effect of microstructure and temperature on toughening mechanisms. *J. Europ. Ceram. Soc.*, **9** (1992) 177–85.